

CHAPTER ONE

PROJECT BACKGROUND

1.1. Background Study

High-temperature pressurized pipelines design requires special attention, as restrained thermal stresses are high. Due consideration should be given to thermal expansion, as stresses in bends of expansion loops are significant. Also, the modeling of the soil-pipe interaction using soil characteristics, especially friction and lateral resistance, is important when analyzing high-temperature pipelines. [1]

Temperature changes along the pipeline is consider as the phenomena of thermal expansion, which will cause the elongation of the pipeline length.

Whatever the pipeline design, it is known that for an ideal round tube or shell, the hydrostatic crushing pressure always is much larger than the actually observed buckling pressure. This drop is due to manufacturing imperfections such as the tube being rendered oval or exhibiting flattened parts, thickness variations etc. [2]

1.2. Problem Statement

Buckling in oil and gas industry is still problematic. In the pipeline there will occur expansion that might be induced by internal pressure and temperature. In recent years, more and more High Pressure and High Temperature (HP/HT) fields are developed using pipelines and steel catenaries' risers. In this design scenario, axial creeping, buckling in

the form of upheaval movements and lateral movements or a combination of both, may take place.

The demand to design static buckling-resistant structures, particularly high-strength alloy structures, has been recognized. The need of a design structures that have to withstand time-dependant dynamic loads, sometimes quite severe, and thus may be susceptible to dynamic buckling. Many classes of problems and many physical phenomena are encompassed by the term dynamic stability. One is associated with the response of structures to the action of oscillating loads i.e. vibration buckling, where the transverse vibration become unacceptably large at critical combination of load amplitude, load frequency and structure damping. Vibration loading will occur when the loading frequency equals twice the natural bending frequency of the column. [2]

So far there is still no technique been implement on how to predict the buckling problem. In real world system with stochastic elements cannot be evaluated analytically, thus a simulation sometimes the only type of investigation which is possible. So that this project will try to do simulation system using catastrophe theory.

1.3. Objective

- The main objective of this project is to apply mathematical catastrophe theory on Pipeline Buckling.
- In order to analyze and study on the importance parameters for predicting the buckling of the oil pipeline the objective is to derive analytical solutions for buckle propagation and fracture of a pipeline subjected to thermal expansion and internal pressure.
- Besides, to have mathematical modeling on MATLAB software.

1.4. Scope of Study

The study of pipeline material and its behavior on sustaining the temperature increasing on the pipeline due to liquid flow in the pipeline. Besides, the catastrophe theory needs to be fully understood in order to simulate or mathematically model the oil pipeline buckling in the MATLAB.

1.5. The relevancy of the project

This project is relevant with applying catastrophe theory on rigid bar beam. As a new approach, the project want to apply the catastrophe theory on the pipeline structure compared to rigid beam.

1.6. Feasibility of Project within the Scope and Time frame

This project was planned to be done in this 2 semester which in first semester all the data need to be collected. The data that need to be collected are the standard size of the oil pipeline, the weight, the material of the pipeline, the behavior of the material, the force exist around the oil pipeline subsea and some mathematical equation related to the buckling and catastrophe theory.

As this second semester the programming is in progress. After the programming done, the author need to analyze the result with the catastrophe theory. Besides the parameters affect the buckling need to be found during the studies.

CHAPTER TWO

LITERATURE REVIEW

2.1. Pipeline buckling causes

A pipeline may experience buckle propagation at high temperature while transferring the liquid (oil) in it. This may cause thermal expansion since the liquid (oil) will be transfer at high temperature condition. The thermal expansion will cause the buckling effect. As the pipeline buckles into a circumferential dog-bone pattern, it undergoes large plastic deformation. Plastic strains at the outer lobes of the buckled pipeline may be very high, exceeding the fracture strain, and result in cracks or leaks in the pipeline. Pipeline rupture due to a propagating buckle is referred to as a wet buckle. [3]

When a pipeline is operated at high internal pressure and temperature, it will attempt to expand and contract for differential temperature changes. Normally the line is not free to move because of the plane strain constraints in the longitudinal direction and soil friction effects. For positive differential temperature it will be subjected to an axial compressive load and when this load reaches some critical value the pipe may experience vertical (upheaval buckling) or lateral (snaking buckling) movements that can jeopardize the structural integrity of the pipeline. In these circumstances, an evaluation of the pipeline behavior should be performed in order to ensure the pipeline structural integrity during operation in such demanding loading conditions. Performing such analysis, the correct mitigation measures for thermal buckling can be taken into account either by acceptance of bar buckling but preventing the development of excessive bending moment, or by preventing any occurrence of bending.

2.2. Thermal expansion

Thermal expansion is the tendency of matter to change in volume in response to a change in temperature. When a substance is heated, its particles begin moving and become active thus maintaining a greater average separation. Materials which contract with increasing temperature are rare; this effect is limited in size, and only occurs within limited temperature ranges. The degree of expansion divided by the change in temperature is called the material's coefficient of thermal expansion and generally varies with temperature.

Common engineering solids usually have thermal expansion coefficients that do not vary significantly over the range of temperatures where they are designed to be used, so where extremely high accuracy is not required, calculations can be based on a constant, average, value of the coefficient of expansion.

For solid materials with a significant length, like rods or cables, an estimate of the amount of thermal expansion can be described by the $\epsilon_{thermal}$ ratio of strain:

$$\epsilon_{thermal} = \frac{(L_{final} - L_{initial})}{L_{initial}} \dots\dots\dots (1)$$

$L_{initial}$ is the initial length before the change of temperature and

L_{final} the final length recorded after the change of temperature.

For most solids, thermal expansion relates directly with temperature:

$$\epsilon_{thermal} \propto \Delta T$$

Thus, the change in either the strain or temperature can be estimated by:

$$\epsilon_{thermal} = \alpha \Delta T$$

where

$$\Delta T = (T_{final} - T_{initial})$$

2.3. Predictive Analytical Models for Global Buckling

The deformed configuration in global buckling analysis is triggered by the initial out-of-straightness (IOS) imposed on the numerical model. The positioning of the IOS can be predicted by the use of analytical models that consider the elastic behavior of the pipe. Good results can be obtained for the global buckling length using this formulation. Nevertheless, due to the elastic-plastic constitutive law applied in the numerical model, in contrast with the elastic formulation of the analytical model, great differences are encountered in the results obtained for the buckling amplitude. These considerations will be exemplified in the following section.

According to [4] the linear differential equation governing the deflected shape of the pipeline has the form (see Fig. 1):

$$y'' + n^2 y + \frac{m}{8}(4x^2 - L^2) = 0 \dots\dots\dots (2)$$

where L or S is the buckle length, $n^2 = P/EI$, P is the axial load at the buckle, E is the elastic modulus, I is the second moment of area of the pipe, $m = w/EI$ for upheaval buckling (vertical mode), w is the selfweight per unit length, and f is the coefficient of friction between the pipe and subgrade.

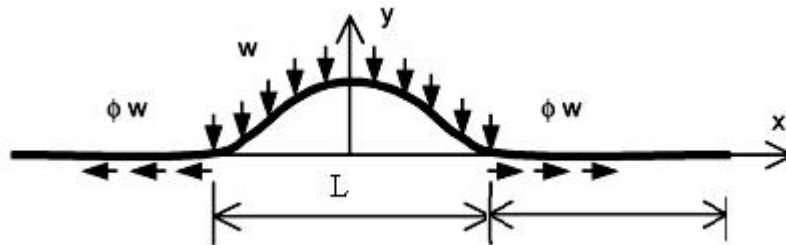


Figure 1: upheaval buckle(vertical mode) consideration

Solving Eq.(2) and applying a compatibility equation that accounts for the reduction in the axial force in the buckle, the following result for the maximum amplitude of the buckle (see Fig. 1) is obtained for upheaval buckling:

$$\bar{y} = 2.408 \times 10^{-3} \frac{wS^4}{EI} \dots\dots\dots(3)$$

The buckle length obtained for the case of a very large coefficient of friction is:

$$\bar{S} = \left[\frac{1.6856 \times 10^6 (EI)^3}{w^2 AE} \right]^{0.125} \dots\dots\dots (4)$$

where A is the cross-sectional area of the pipe.

For snaking buckling (lateral mode) shown in Fig. 2, the differential equation governing the deflection is the same as Eq.(2), except that $m=fw/EI$. For snaking buckling the following results are obtained:

$$\bar{y} = 1.047 \times 10^{-2} \frac{\phi w L^4}{EI} \dots\dots\dots (5)$$

$$\bar{S} = \left[\frac{2.7969 \times 10^5 (EI)^3}{(\phi w)^2 AE} \right]^{0.125} \dots\dots\dots (6)$$

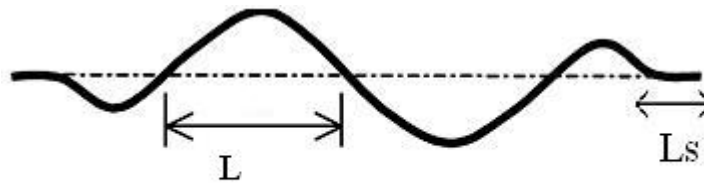


Figure 2: snaking buckling (lateral mode) shape

In this analysis it is assumed that the cross section of the pipe remains circular. This is true at least in the initial stages of buckling, although the global buckling responses discussed here may lead to local buckling and failure of the pipe by yielding and

ovalization. More details about this derivation can be seen in Hobbs (1984). In this work, only the derived equations for buckle length and amplitude are presented as they are of interest to predict the pipe global buckling configuration. [4]

The magnitude of axial load in the pipe wall depends on many factors. As well as the mechanical properties of the line and its weight coat, the axial force is a function of the initial tension at a seabed just after laying, the pressure difference across the pipe wall and temperature variation due to hot oil passing through the line. These factors interact with seabed geometry and frictional or trench backfill effects or both as well as the influence of end restraints in shorter lines. Akten has treated some effects of partial end restraint at a platform tie-in and Yen et al. have described some analogous phenomena in land based pipelines. Finally, the previous loading history and time dependent changes due to scour, currents and tides are so relevant. [5, 6]

Thus it is extremely difficult to say with any certainty what axial force exists at any point in a given pipeline at a given time. Nonetheless, two major causes of compressive forces can be identified, arising from the restraint of the strains associated with thermal and internal pressure loadings. With oil and gas temperatures potentially up to 180°F (100°C) above water temperature and operating pressure over 1450 lb/in² (10 N/mm²) these effects can produce very significant forces indeed in a long line where the necessary frictional force can develop between pipe and seabed, or in shorter lines with effective end restraints. Denoting the cross-sectional area of the pipe by A, Young's Modulus by E, the coefficient of linear thermal expansion by α and the temperature change by T, the force P_0 created by full restraint of thermal expansion is simply,

$$P_0 = EA\alpha T \dots\dots\dots (7)$$

The free axial strain, ϵ , due to a positive pressure difference p between the oil and the sea is given in terms of the well-known thin wall axial and hoop stresses in the pipe by

$$\epsilon = 1/E (pr/2t - \nu pr/t) \dots\dots\dots (8)$$

in which ν is Poisson's ratio, and t and r are the pipe wall thickness and radius respectively. Then, if ϵ is completely restrained, the axial compressive force generated and available to participate in buckling is

$$P_0 = EA\epsilon = Apr/t (0.5-\nu) \dots\dots\dots (9)$$

This paper addresses two possible responses to the compressive force generated. Both involve significant bending of the initially straight pipeline, similar to the bending deformation occurring in the elastic (Euler) buckling of an axially loaded column as its critical load is approached. As in a long column fabricate from a circular hollow section, the cross section of the pipe remains circular, at least in the initial stages of buckling, although the responses discussed here may well lead to pipe overstress and local failure by yielding and ovalization. The initial absence of gross cross-sectional distortion may be contrasted with the situation in a propagating buckle triggered by excessive bending and external pressurization during laying operations. The first buckling mode (figure 1) addressed here involved part of the line lifting itself vertically from the seabed, while the second (Figure 2) results in various snaking lateral movements on the horizontal plane against frictional resistance. [7, 9]

From equation (2);

$$y = \frac{m}{n^4} \left(\frac{-\cos nx}{\cos \frac{nL}{2}} - \frac{n^2 x^2}{2} + \frac{n^2 L^2}{8} + 1 \right) \dots\dots\dots (10)$$

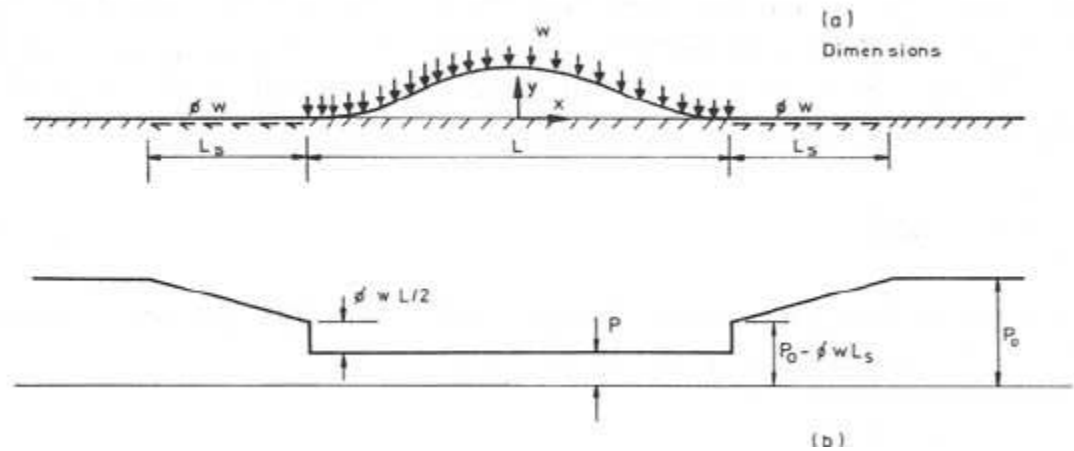


Figure 3: details of vertical buckle

The unknown length of buckle L is then determined from the condition that the slope at the ends of the buckle should be zero. This yields

$$\tan \frac{nL}{2} = \frac{nL}{2} \dots\dots\dots (11)$$

Or as lowest root

$$nL=8.9869 \dots\dots\dots (12)$$

the next step is to compare the axial load P in the buckle with the axial load P_0 well away from the buckle. P is clearly less than P_0 because of the extra length round the buckle compared to L itself. The drop in force is not as large as would be expected at the first glance because two adjacent length of pipe L_s slide on towards the buckle-giving the axial force distribution. The discontinuities in this distribution at each lift-off point are associated with concentrated vertical reactions of $0.5wL$ which occur there.

$$P = 80.76 \frac{EI}{L^2} \dots\dots\dots (13)$$

$$P_0 = P + \frac{wL^4}{EI} [1.597 \times 10^{-5} EA \Phi w L^5 - 0.25(\Phi EI)^2]^{1/2} \dots\dots\dots (14)$$

In which ϕ is the coefficient of friction between pipeline and subgrade. The maximum amplitude of the buckle

$$\hat{y}' = 2.408 \times 10^{-3} \frac{wL^4}{EI} \dots\dots\dots (15)$$

And the maximum bending moment at $x=0$, is

$$\hat{M} = 0.06938wL^2 \dots\dots\dots (16)$$

While the slope is

$$\hat{y}' = 8.657 \times 10^{-3} \frac{wL^3}{EI} \dots\dots\dots (17)$$

This last result is useful for checking the validity of the small slope assumption on particular numerical cases, i.e. conventionally $\hat{y}' \leq 0.1$ for “small” slopes. A further result of practical interest is the size of the slipping length adjacent to the buckle,

$$L_s = \frac{P_0 - P}{\Phi w} - 0.5L \dots\dots\dots (18)$$

Thus the minimum theoretical distance between the centers of two adjacent but independent vertical buckles is

$$L + 2L_s = \frac{2P_0 - P}{\Phi w} \dots\dots\dots (19)$$

Equation (14) is awkward and may be compared with the result for a very large coefficient of friction (i.e., $L_s=0$)

$$P_0 = 80.76 \frac{EI}{L^2} + 1.597 \times 10^{-5} \frac{w^2 AEL^6}{(EI)^2} \dots\dots\dots (20)$$

It is easy to show that Equation (20) has a minimum at a buckle length

$$\bar{L} = \left[\frac{1.6856 \times 10^6 (EI)^3}{w^2 AE} \right]^{0.125} \dots\dots\dots (21)$$

CHAPTER THREE

METHODOLOGY

3.1. Research Methodology

After gone through all the mathematical equation, the part of mathematical modeling need to be proceed which the equation found are arranged to be used in the problem..

3.2. Project Activities

Running the MATLAB software in order to get the mathematical modeling of the buckling. Once the temperature and axial force are found, it can be discuss due to thermal expansion which lead to compressive load over the pipeline that are fix at both ends.

3.2.1 Mathematical Modeling

From the experiment observed by Roger E.Hobbs the lateral modes once more, it was assumed that the families of decaying trigonometric curves were all initial imperfection generated variants of one fundamental constant amplitude periodic curve. In other words, it was assumed that an initially perfect pipe would buckle into an indefinite series of half waves. This assumption has the computational advantages that the nodes of the half wave pattern do not slide parallel to the axis of the pipe and, more importantly, can be made to satisfy lateral equilibrium.

The displacement boundary conditions are unchanged but for the zero slope condition at $x=\pm L/2$ which is replaced by a shear force condition at the same location.

$$\tan \frac{nL}{2} = 0 \dots\dots\dots (22)$$

Or as the lowest non-trivial root

$$nL=2\pi \dots\dots\dots (23)$$

Compatibility then requires that

$$P_0 - P = \frac{AE}{L} \int_{-L/2}^{L/2} \frac{1}{2} y'^2 \dots\dots\dots (24)$$

That is: the reduction in axial force in the buckle equals the product of the axial stiffness and the extension round the curve. This leads to the following results for infinite lateral buckling mode

$$P = 4\pi^2 \frac{EI}{L^2} \dots\dots\dots (25)$$

$$P_0 = P + 4.7050 \times 10^{-5} AE \left(\frac{\Phi w}{EI} \right)^2 L^6 \dots\dots\dots (26)$$

For computational use, it is noted that this equation has a minimum at

$$\bar{L} = \left[\frac{2.7969 \times 10^{-5} (EI)^3}{(\Phi w)^2 AE} \right]^{0.125} \dots\dots\dots (27)$$

The maximum amplitude of the buckle

$$\hat{y} = 4.4485 \times 10^{-3} \frac{\Phi w}{EI} L^4 \dots\dots\dots (28)$$

The maximum bending moment, at $x=0$, is

$$\hat{M} = 0.05066\Phi wL^2 \dots\dots\dots (29)$$

while maximum slope is;

$$\hat{y}' = 0.01267 \frac{\Phi w}{EI} L^3 \dots\dots\dots (30)$$

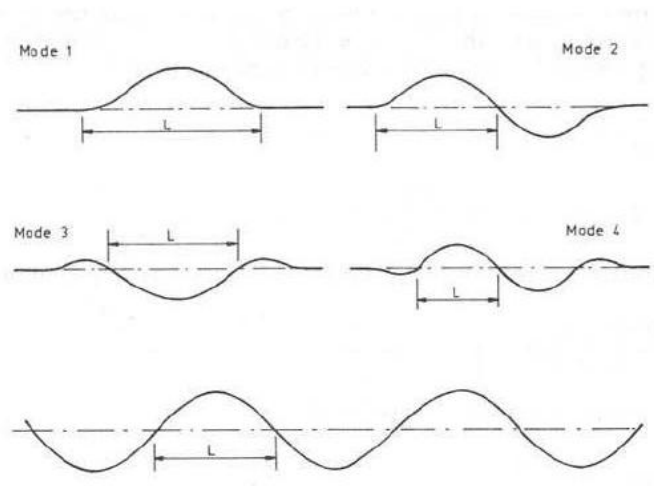


Figure 4: lateral buckling modes

From the studies of lateral mode 1 (upheaval/vertical) the lack of lateral equilibrium at the ends of the buckles were observed and an assumption is made as the mode 3 (snaking) exist with a smaller lack of equilibrium at its ends was likely developed as figure 4. [8]

As the assumption is made, he found the higher mode, confirming buckling would be initiated at lower axial force for a given out-of-straightness than necessary for lateral buckling mode. [9]

Martinet and Kerr's studies helps the assumption proven with giving out the formulas for modes 1-4 (figure 4). Taking the half wavelength of the most significant part of the buckle as L in each case (Fig 4), and using the constants of Table 2, the reduced axial force within the buckle is given by

$$P = k_1 \frac{EI}{L^2} \dots\dots\dots (31)$$

$$\text{Then } P_0 = P + k_3 \Phi w L \left[\left(1.0 + k_2 \frac{AE \Phi w L^5}{(EI)^2} \right) - 1.0 \right] \dots\dots\dots (32)$$

The maximum amplitude of the buckle relative to the original axis is

$$\hat{y} = k_4 \frac{\Phi w}{EI} L^4 \dots\dots\dots (33)$$

While the maximum bending moment \hat{M} is

$$\hat{M} = k_5 \Phi w L^2 \dots\dots\dots (34)$$

3.3. Tools and software

By computing the equation in MATLAB software to have the curve of the buckling which shows the lateral displacement along the axial coordinates.

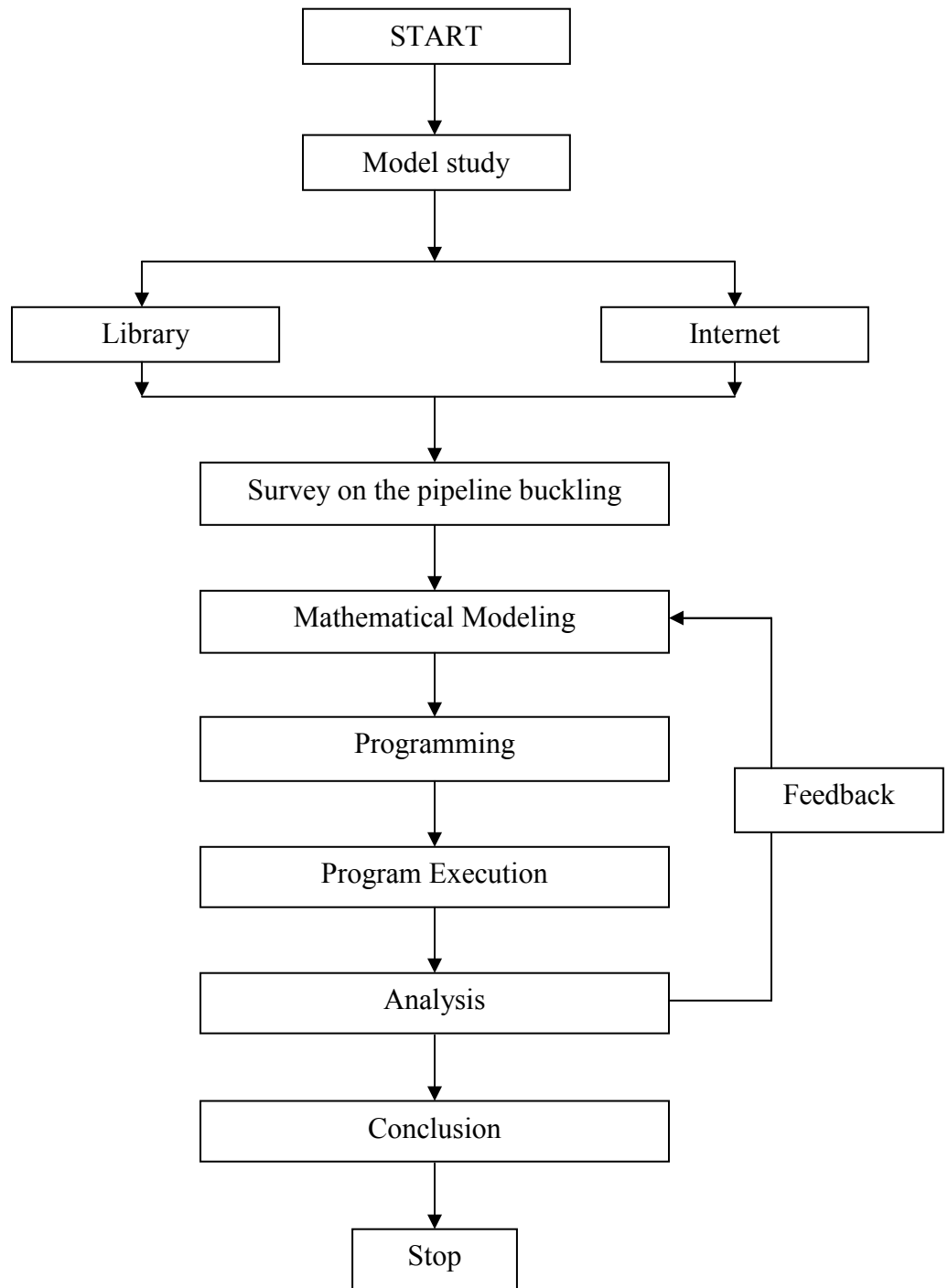


Figure 3: Execution of flow chart

3.4. Gantt Chart

Miles stone for Final Year Presentation Semester 2

No.	Activities	Week No / Date													
		1	2	3	4	5	6	7	8	9	10	11	12	13	14
1	Programming of the MATLAB														
2	Submission of progress report														
3	programming on the MATLAB														
4	Submission of progress report 2														
5	seminar														
6	analysis and conclusion of programming output														
7	poster exhibition														
8	submission of dissertation final draft														
9	Oral Presentation														
10	submission of dissertation(hardbound)														

CHAPTER FOUR

RESULT

4.1. Finding and Data Gathering

In order to solve the equation (2) from Hobbs, a program in the MATLAB had been tried. All the data are calculated which are:

Dimension of pipe	Size of pipe dimension
Length	2km
Diameter	24inch
Thickness	0.5inch

Table 1: Pipeline dimension

Weight per length, w is calculated as:

$$\begin{aligned}w &= 10.68t \times (D - t) \\ &= 10.68(0.5) \times (24 - 0.5) \\ &= 125.49 \text{ lb/ft} \\ &= 125.49 \times 1.49 \\ &= 186.98 \text{ kg/m}\end{aligned}$$

$n^2 = P/EI$ where P is the axial load.

Area:

$$\begin{aligned}A &= \pi (D^2 - d^2)/4 \\ A &= \pi (0.6096^2 - 0.5842^2)/4 \\ A &= 0.02382 \text{ m}^2\end{aligned}$$

Mass, m is calculated based on:

$$\begin{aligned}m &= w/EI \\ m &= 125.49 / (200000 \text{ MPa} \times 6.6 \times 10^{-5}) \\ &= 1.42 \times 10^{-5} \text{ s}^2 \text{ m}^{-4}\end{aligned}$$

Thus;

$$y'' + 7.33 \times 10^{-9} y + 1.77 \times 10^{-6} (4x^2 - L^2) = 0$$

x variable varies from 0.2 to 2km of the pipeline length.

4.1.1 Thermal expansion

Vertical mode-high friction coefficient

The temperature rise generates the axial force in equilibrium with buckle lengths and amplitudes, and the coefficient of linear thermal expansion has been taken as $11 \times 10^{-6}/^{\circ}\text{C}$ for this purpose.

By solving equation (20) which will give the tabulated value of compressive load exert by the temperature changes through the pipeline.

No.	Force, F				
1-5	258.731	633.931	1009.131	1384.331	1759.531
6-10	2134.731	2509.931	2885.131	3260.331	3635.531
11-15	4010.731	4385.931	4761.131	5136.331	5511.531
16-20	5886.731	6261.931	6637.131	7012.331	7387.531

Table 3: axial/compressive force exert

Vertical mode-real friction coefficients

Using the same method, but the equation of the axial force is used from equation (14) the temperature changes with the axial force relation are solved.

For this type of buckling mode, the friction coefficient is varies from 0.3 to 0.7.

Lateral modes-infinite mode

The calculation is done same as vertical mode only the equation is change. For the situation equation (26) is used for the relation of axial force and the buckling size.

The amplitude for lateral buckling is calculated using equation (28).

4.2 Result

Graph pattern of vertical buckling mode. Here is for high friction coefficient condition see appendix 2,3

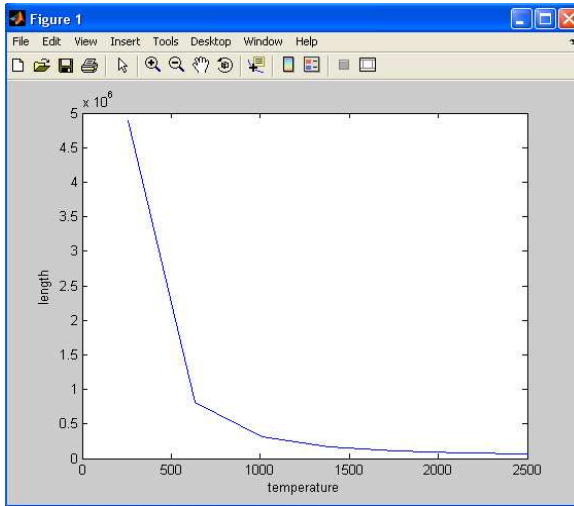


Figure 5: Temperature vs buckling length

4.2.1 Lateral mode

4.2.1.1 At friction coefficient =0.3 see appendix3, 4 for coding simulation and calculation

The calculation of the buckle length, L from the simulation:

$$0.5L_{max} \leq L \leq 1.5L_{max}$$

No.	Length, L				
1-5	1396.452	1536.452	1676.452	1816.452	1956.452
6-10	2096.452	2236.452	2376.452	2516.452	2656.452
11-15	2796.452	2936.452	3076.452	3216.452	3356.452
16-20	3496.452	3636.452	3776.452	3916.452	4056.452

Axial force calculated, P

No.	Force, P				
1-5	8.06E+12	1.43E+13	2.41E+13	3.9E+13	6.09E+13
6-10	9.23E+13	1.36E+14	1.96E+14	2.76E+14	3.82E+14
11-15	5.2E+14	6.97E+14	9.21E+14	1.2E+15	1.55E+15
16-20	1.99E+15	2.51E+15	3.15E+15	3.92E+15	4.84E+15

Temperature varies from the force, T:

No.	Temperature, T				
1-5	1.07E+12	1.89E+12	3.2E+12	5.17E+12	8.08E+12
6-10	1.22E+13	1.8E+13	2.59E+13	3.66E+13	5.06E+13
11-15	6.89E+13	9.23E+13	1.22E+14	1.59E+14	2.06E+14
16-20	2.63E+14	3.33E+14	4.18E+14	5.2E+14	6.42E+14

Buckling amplitude results, \hat{y} :

No.	Buckling Amplitude, \hat{y}				
1-5	31.04694	45.49784	64.48806	88.88133	119.6167
6-10	157.7083	204.2458	260.3941	327.3931	406.5583
11-15	499.2803	607.025	731.3336	873.8226	1036.184
16-20	1220.184	1427.665	1660.546	1920.818	2210.55

4.2.1.2 At friction coefficient =0.5

The calculation of the buckle length, L from the simulation:

No.	Length, L				
1-5	1229.034	1354.034	1479.034	1604.034	1729.034
6-10	1854.034	1979.034	2104.034	2229.034	2354.034
11-15	2479.034	2604.034	2729.034	2854.034	2979.034
16-20	3104.034	3229.034	3354.034	3479.034	3604.034

Axial force calculated, P

No.	Force, P				
1-5	798996.3	658284.1	551716.8	469078.3	403706.2
6-10	351105	308152.7	272625.8	242906.4	217794.5
11-15	196384.6	177983.2	162052	148167.9	135994.5
16-20	125262	115751.6	107284.6	99713.74	92916.87

Temperature varies from the force, T:

No.	Temperature, T				
1-5	1.38E+12	2.47E+12	4.19E+12	6.81E+12	1.07E+13
6-10	1.62E+13	2.4E+13	3.47E+13	4.91E+13	6.81E+13
11-15	9.28E+13	1.25E+14	1.65E+14	2.16E+14	2.8E+14
16-20	3.58E+14	4.53E+14	5.69E+14	7.09E+14	8.77E+14

Buckling amplitude results, \hat{y} :

No.	Buckling Amplitude, \hat{y}				
1-5	31.04694	45.73846	65.11424	90.07778	121.6123
6-10	160.7808	208.726	266.6702	335.9157	417.8443
11-15	513.9176	625.677	754.7435	902.8179	1071.681
16-20	1263.192	1479.293	1722.001	1993.418	2295.721

For friction coefficient $\varphi=0.7$ the pattern of the result is almost same with $\varphi=0.3$ and 0.5 .

see appendix 4

CHAPTER FIVE

DISCUSSION

For vertical/upheavel buckling mode the temperature changes which cause the compressive load/axial force given a high slope of temperature change, T against buckling length, L which shows it is slightly hard to buckle when the coefficient friction high.

The lateral mode becomes possible at a smaller temperature change than the vertical mode for realistic friction coefficient. This feature is confirmed by small scale experiment and practical experience. An unburied line will snake laterally, while a buried line will burst out of the seabed Once buried line has lifted, an interaction with lateral mode will occur, as the buckle itself now has no lateral restraint ($\Phi=0$). Alternatively the buckle may roll or twist laterally.

In a finite elements analysis in which the buckle wave-length is constrain to be the same as the wavelength of the initial imperfection and a limited length of track is considered so that unloading into the buckle is restricted. In small scale model substantial wavelength changes do occur during buckling, and the writer feels that more work on the effects on initial imperfection is needed. It is clear that such work will be based on numerical rather than numerical studies. [9]

All the analysis shows there will always have imperfection in buckling condition which some might cause by the environment. This is what we can said as a catastrophic failure which means a natural phenomena. As the studies had been done we can said that the

weather worsen involuntary large radius curve may be induced at the seabed by laybarge motion but it is no practical to lay the line to specified radii. This can affect the buckling of the pipeline occur suddenly. As found in the numerical presented earlier, mode 3 seems to be associated with rather larger amplitudes and bending stress. Which of these three modes develop in a particular case is thought to be determine by initial imperfection in a given pipeline.

A warning point should be made about the analyses of mode 3 and 4, in particular. It is recognized that they contain an approximation which will lead to an over estimate of the amplitude. In the analyses it has being assumed that the axial force P is constant through the entire buckle, which respect to the thermal expansion of the oil temperature flows thorough it in spite of the inward movement from the adjacent unbuckled pipeline.

CHAPTER SIX

CONCLUSION AND RECOMMENDATION

CONCLUSION

Two potential buckling mechanisms in pipelines subjected to axial compression have been identified and analyzed which confirm half of the project objective. It is found that horizontal snaking modes occur at a lower axial load than vertical mode, and horizontal mode is therefore dominant unless lateral restraint is provided by trenching when an interactive buckling mode becomes possible. Full account has been taken of friction between the pipe and the ground in the vertical mode, relying on two independent but formally identical references on the buckling of rail tracks and crane rails. An analysis of lateral mode involving an infinite sequence of half waves with fully developed lateral friction has been presented and compared with earlier work on isolated buckles over a shorter length which involves longitudinal as well as lateral sliding.

The effects of imperfections, unloading and reloading are discussed and it is concluded that further numerical work on the effect of initial imperfections would be valuable. The theoretical solutions are illustrated by numerical results of typical pipeline.

RECOMMENDATION

From all the studies, we should improve it as a tool to monitor the buckling occurrence using the mathematical modeling and simulation of a software. This can help the oil and gas industry minimize the maintenance cost for once the buckling occurs.

References

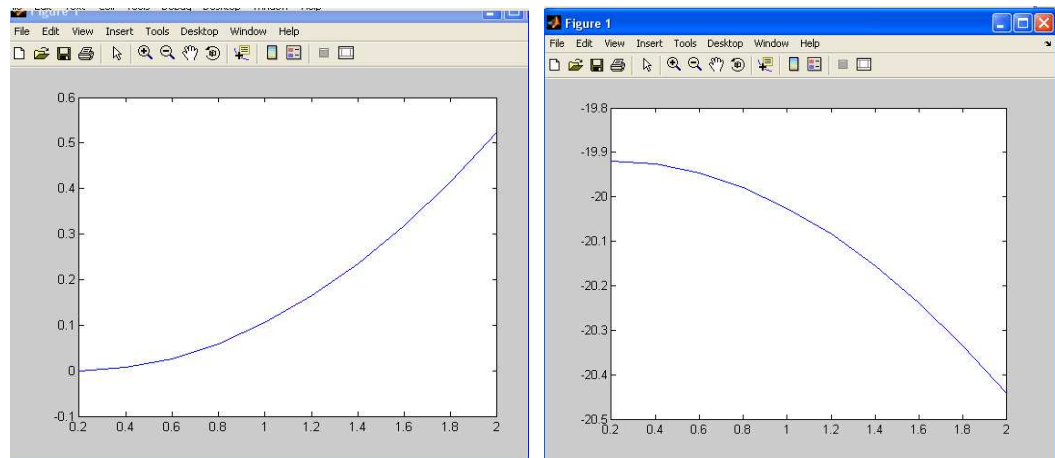
- [1] American Mathematical Society,
<http://www.ams.org/featurecolumn/archive/cusp3.html> , (August 21, 2009.)
- [2] Double-shell pipeline exhibiting improved buckling strength,
<http://www.freepatentsonline.com/6568431.html> (September 6, 2009)
- [3] Double-shell pipeline exhibiting improved buckling strength,
<http://www.freepatentsonline.com/6568431.html> (September 6, 2009)
- [4] R. A. Einsfeld^I; D. W. Murray^{II}; N. Yoosef-Ghodsi^{III}, “Buckling analysis of high-temperature pressurized pipelines with soil-structure interaction”, *Journal of the Brazilian Society of Mechanical Sciences and Engineering*, J. Braz. Soc. Mech. Sci. & Eng. vol.25 no.2 Rio de Janeiro Apr./June 2003
- [5] Akten,H. T., “New Developments in Submarine Pipeline in Place Stability Analysis,” *Proceeding of Arctic/Offshore/Deepsea System Symposium*, American Society of Mechanical Engineers, New Orleans 1982.
- [6] Yen, B. C., Tsao, C. H., and Hinkle, R. D., “Soil-Pipe Interaction of Heated Oil Pipelines,”*Journal of Pipeline Division*, ASCE, Vol. 107, No. Tel, Jan 1981,pg 1-14
- [7] Palmer, A. C., and Martin, J. H., “Buckle Propagation in Submarine Pipelines,” *Nature* Vol.254 Mar., 1975 pg. 46-48
- [8] Martinet, A., “Buckling of Tracks without Joints on Ballast and Very Long Rail ,”pg. 212
- [9] Hobbs, R. E., “Solution for Pipeline Tie-In and Repair Problems,” *Proceeding Second Symposium on Offshore Mechanics and Arctic Engineering*, American Society of Mechanical Engineers, Houston, Tex., 1983 pg. 538-552

Appendix 1

For first trial of computation the mathematical modeling in the MATLAB:

```
Editor - C:\Program Files\MATLAB71\work\nana.m
File Edit Text Cell Tools Debug Desktop Window Help
x=[0.2 0.4 0.6 0.8 1.0 1.2 1.4 1.6 1.8 2.0];
b=7.33*10^-9;
T1=-60;
T2=[-60 -40 -20 0 20 40 60 80 100 120];
s=0.508*(T2-T1);
c=(1.77*10^-6)*((4*x.^2)-(s.^2))
y1=-b+sqrt((b^2)-(4*c))
y2=-b-sqrt((b^2)-(4*c))
```

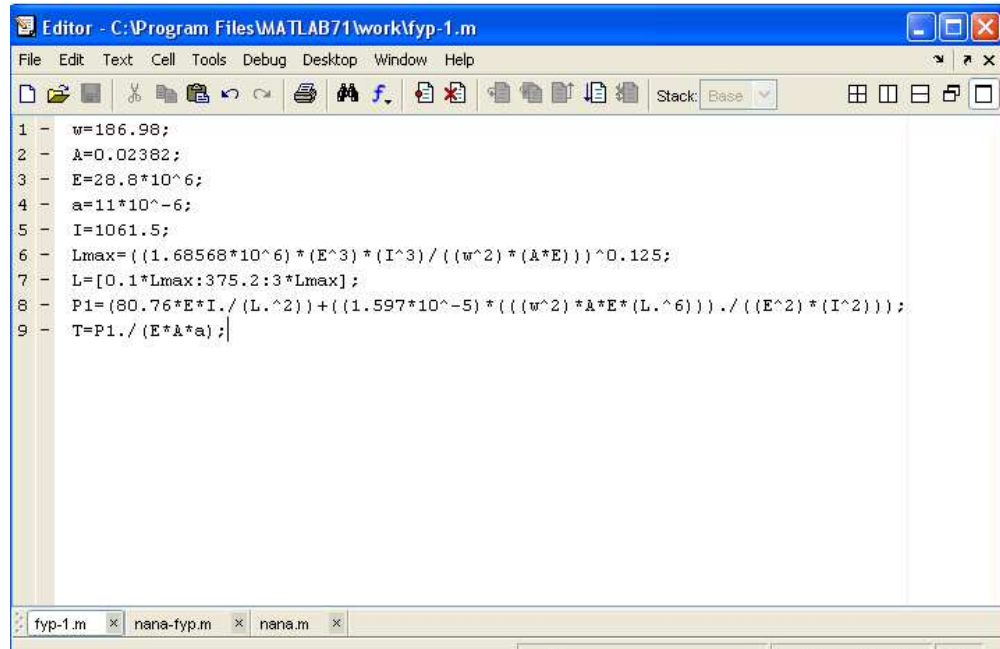
Coding



Lateral displacement against axial coordinate

Appendix 2:

Coding for vertical mode-high friction coefficient:



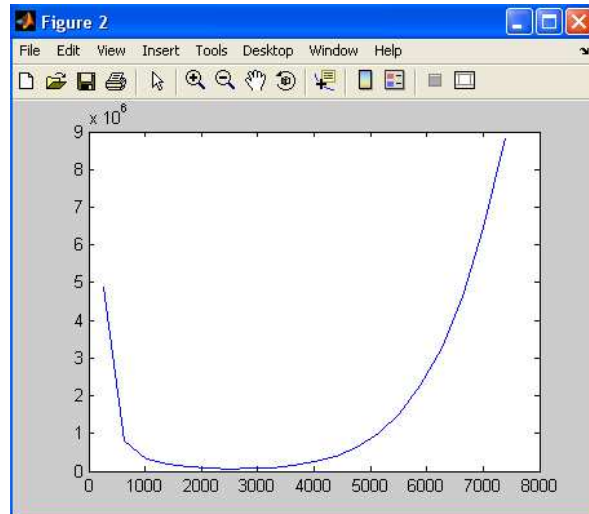
The image shows a screenshot of a MATLAB Editor window. The title bar reads "Editor - C:\Program Files\MATLAB71\work\fyp-1.m". The menu bar includes "File", "Edit", "Text", "Cell", "Tools", "Debug", "Desktop", "Window", and "Help". The toolbar contains various icons for file operations and editing. The main editing area contains the following MATLAB code:

```
1 - w=186.98;  
2 - A=0.02382;  
3 - E=28.8*10^6;  
4 - a=11*10^-6;  
5 - I=1061.5;  
6 - Lmax=(1.68568*10^6)*(E^3)*(I^3)/((w^2)*(A*E))^0.125;  
7 - L=[0.1*Lmax:375.2:3*Lmax];  
8 - P1=(80.76*E*I./(L.^2))+((1.597*10^-5)*((w^2)*A*E*(L.^6))./((E^2)*(I^2)));  
9 - T=P1./(E*A*a);
```

The status bar at the bottom shows the current file "fyp-1.m" and other open files "nana-fyp.m" and "nana.m".

Appendix3

Vertical mode



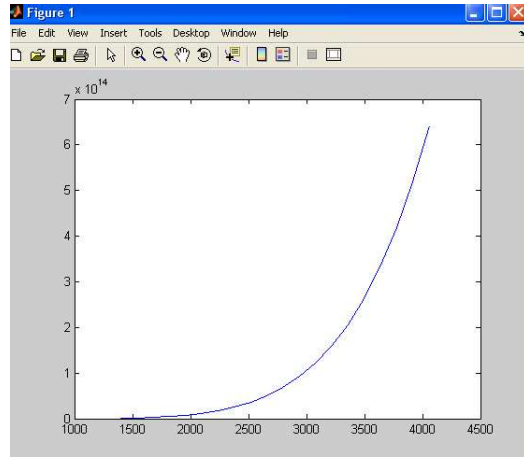
Lateral mode

Coding

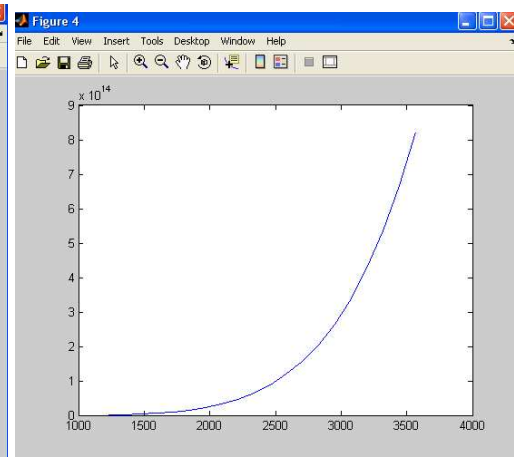
```
Editor - C:\Program Files\MATLAB71\work\fy3lateral modes.m
File Edit Text Cell Tools Debug Desktop Window Help
|
|
|
1 - w=186.98;
2 - A=0.02382;
3 - E=28.8*10^6;
4 - a=11*10^-6;
5 - I=1061.5;
6 - P=4*(pi^2)*E*I./(L.^2)
7 - %f between 0.3 to 0.7
8 - %try run at f=0.3,0.5,0.7
9 - %a is referring to thermal coefficient
10 - >> Lmax=(2.7969*10^5)*((E*I)^3)/((f.^2)*w^2*A*E)^(0.125)
11 - L=[0.5*Lmax:140:1.5*Lmax]
12 - P1=P+(4.705*10^5*A*E*((f.*w)./(E*I))^2)*L.^6)
13 - T=P1./(E*A*a)
14 - ymax=4.4495*10^-3*f*w*(L.^4)/(E*I)
15
fy2vertical mode.m x fy3lateral modes.m x
script Ln 1 Col 1 OVR
```

Appendix4

Graph



Friction coefficient=0.3



friction coefficient=0.5